Journal of Applied Electrochemistry **30**: 29–34, 2000.

Impedance spectroscopic study for the initiation of passive film on carbon electrodes in lithium ion batteries

C.R. YANG, J.Y. SONG, Y.Y. WANG* and C.C. WAN
Department of Chemical Engineering, National Tsing-Hua University, Hsinchu 300, Taiwan
*(*author for correspondence, e-mail: yywang@faculty.nthu.edu.tw)*

Received 14 May 1997; accepted in revised form 9 December 1998

Key words: a.c.-impedance, lithium-ion battery, organic electrolyte, passive film

Abstract

The formation of passive film at the interface between the mesocarbon microbeads (MCMB) electrode and the organic electrolyte in a lithium-ion battery during the initial period of intercalation was investigated by a.c.-impedance spectroscopy. An equivalent-circuit model consisting of five parallel RC-circuits in series combination was adopted for the curve-fitting analysis of the obtained impedance spectra. The results indicated that both the total interfacial resistance and the passive film thickness increased with decreasing intercalation potential in the ethylene carbonate (EC) or dimethyl carbonate (DMC) single-solvent system, whereas an opposite trend was observed in the system containing diethyl carbonate (DEC) only. In addition, the total interfacial resistance was clearly affected by the porous structure of the passive film in a single-solvent system. In binary solvent systems such as EC/DEC and EC/DMC, on the other hand, the effect of the porous structure on the total interfacial resistance was negligible. The total interfacial resistance and the passive film thickness were also smaller in these systems than those in single-solvent systems. Finally, the variation of the total interfacial resistance and of the passive film thickness in the EC/DEC (or EC/DMC) system were also found to be similar to those in the parent DEC (or DMC) system during intercalation.

1. Introduction

Carbonaceous materials are widely employed as the anodes in lithium-ion batteries. Much effort has been devoted to the improvement of the reversible performance of these insertion materials [1–7]. Although the structure of carbon itself plays a vital role in the lithium intercalation/deintercalation process, the passive film, or the solid electrolyte interphase (SEI), formed on the surface of the carbon electrode is equally important [8–13]. The significance of the passive film in primary and secondary batteries cannot be overestimated. It determines the safety, power capability, shelf life and cycle life of a battery. The morphology (compact or porous), thickness, ionic transference number and conductivity of the passive films are some of the most critical factors affecting the performance of carbon electrodes.

When a carbon electrode is polarized to low potentials, electrolyte species will undergo reduction at potentials higher than that of the lithium insertion process. Passive films will consequently precipitate on the carbon surface in a way resembling that of a lithium electrode. If these passive films are fully developed and form compact and ion-conductive layers which completely isolate the carbon active materials from the electrolyte solution before it attains the insertion potential, the electrode can be, at least kinetically, stabilized.

Impedance spectroscopy has been routinely utilized to study the passive films formed on the surface of an electrode. Aurbach and Zaban [14, 15] used this technique to investigate the SEI formation on lithium anodes in contact with various organic electrolytes. They suggested an SEI structure which consists of five different consecutive layers for reflecting the variations in composition and morphology of the multilayered SEI, and delineated this model by a series of four to five parallel RC circuits representing the capacitance and resistance of each layer. The thickness of each layer of the SEI could consequently be calculated with some assumptions introduced. Besenhard [10] used a simpler equivalent-circuit model to calculate the passive film resistance. Takami [16] also employed a similar model to estimate the diffusion coefficient of lithium ion D_{Li^+} within the carbon electrode.

Most of the studies mentioned above were performed in a single solvent system. A comparative study of the passive film in electrolyte systems using ethylene carbonate (EC), diethyl carbonate (DEC), or dimethyl carbonate (DMC) separately, or in combination as the solvent(s) is still rarely found. Furthermore, most impedance studies were focused on the characteristics

of the passive film after numerous charge–discharge cycles. However, the way in which the passive film grows and changes in structure during the initial period should also be of interest. In this study, the impedance spectroscopy of passive films during the initial cycling stage in various single or binary solvents based on EC, DEC and DMC was examined. The interaction of two solvents in a binary solvent system and their effects on the passive film was also discussed.

2. Experimental details

A MCMB (mesocarbon microbeads) carbon electrode containing 10% polyvinylidene fluoride (PVDF) binder was used as the working electrode while the counter and reference electrodes were made of metallic lithium. The average particle size and surface area of the MCMB powder were 6 μm and 2.89 $m^2\ g^{-1}$, respectively. The dimensions of both the working and counter electrodes were 2 cm × 2 cm square sheets. The separator was Celgard PP (polypropylene). The electrolyte systems studied were 1 M $LiPF_6$ in the following solvent or solvent combinations: EC, DEC, DMC, EC/DEC (1:1 v/v), and EC/DMC (1:1 v/v). All the solvents were battery-grade chemicals from the Tomiyama Corp., Japan, and were used as received. The water contents of these solvents were also verified to be less than 10 ppm via the Karl Fischer titration test. The temperature of the cell was controlled at 25 ± 0.5 °C.

The cells were tested on a charge–discharge unit (Hokuto Denko, model HJ-201B). In this investigation, lithium ions were intercalated into the carbon electrode by a discharging process. The discharging current density was fixed at 0.25 mA cm^{-2} until the cell potential reached the designated cutoff potentials, for example, 0.5, 0.2, and 0.05 V vs Li/Li^+. Each cutoff point represents a different extent of intercalation. At first, the cells were kept at the open-circuit condition for one hour before performing impedance tests such that the equilibrium of the cells could be ensured. Then, a.c. impedance analyses were performed on the cells by a Solartron 1286 electrochemical interface coupled to a Solartron 1255 frequency response analyser (FRA) driven by the Zplot software from Scribner Assoc. The frequency ranged from 100 000 to 0.01 Hz and the a.c. modulation was controlled at 5 mV. Finally, the obtained impedance data were analyzed according to the proposed equivalent-circuit model with the aid of Zsim software (Scribner Associates) based on Macdonald's CNLS programs [17].

3. Results and discussion

According to Aurbach [12, 18, 19], an equivalent-circuit model consisting of a series of five parallel RC circuits can adequately simulate the interface between the metallic lithium electrode and the organic electrolyte. However, similar methodology has rarely been applied to a porous carbon electrode. Therefore, we adopted that concept to analyse the interface between the surface of the MCMB electrode and the electrolyte. Since a carbon electrode is porous in nature, its effective area is difficult to estimate accurately. Hence, we adopted Aurbach's method of choosing the geometric area as the characteristic area.

Figure 1 depicts the equivalent-circuit model with five parallel RC circuits in series. We attribute R_1, R_2 and R_3 to the resistances for Li^+ migration through the inner three layers of the passive film near the MCMB surface. The sum of these three terms represents the overall inner resistance of the passive film (R_i). Consequently, C_1, C_2 and C_3 can be attributed to the corresponding film capacitances for R_1, R_2 and R_3, respectively. R_4 denotes the resistance of the outer layer of the passive film near the electrolyte and C_4 is the corresponding capacitance of this layer. R_5 represents the charge-transfer resistance at the interface between MCMB particles and the passive films and C_5 the double-layer

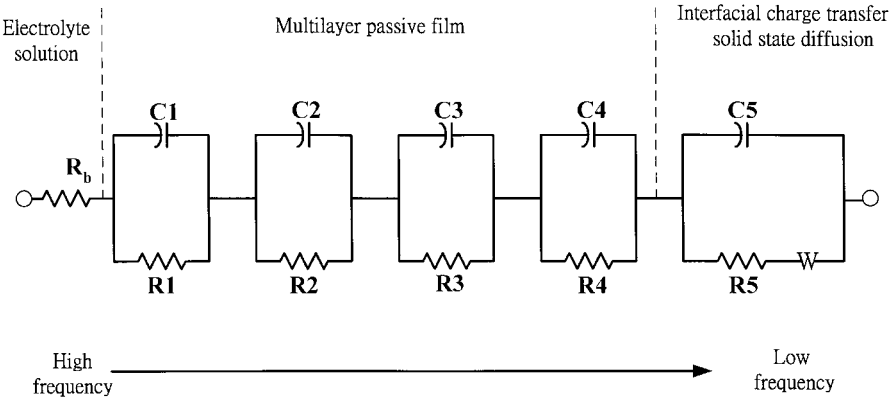

Fig. 1. Equivalent circuit model of the passive film on a carbon electrode of a lithium-ion battery. R_b denotes the bulk electrolyte resistance. R_1, R_2, R_3 and R_4 represent the resistances for Li^+ migration through each layer of the passive film whereas C_1, C_2, C_3 and C_4 are the corresponding layer capacitances, respectively. R_5 is the charge-transfer resistance at the interface between electrode particles and the passive film. C_5 is the double-layer capacitance. W is the Warburg impedance accounting for the solid-state diffusion of Li^+ in the electrode bulk.

capacitance. Finally, R_b denotes the bulk solution resistance and W is the Warburg element accounting for the solid state diffusion of lithium ions in the electrode bulk.

For a better understanding of the intercalation process, Zsim Software (Scribner Associate, USA) developed by Macdonald [17] was employed in the curve-fitting analysis of the impedance spectra in order to estimate the value of each term in the model. Figures 2–6 show the Nyquist plots for various electrolyte systems. Solid symbols within the figures are the experimental data, all of which closely correspond to the fitting curves. Tables 1 and 2 summarize the numerical values for all terms in the model and the correlated thickness of the passive films in single and binary solvent systems, respectively.

Figure 2 illustrates the variation of typical Nyquist plots obtained at four selected cutoff potentials in the first intercalation step for the EC/1 M $LiPF_6$ electrolyte system. Figure 2(a–d) each represent a different open circuit voltage (OCV) at 3.1, 0.64, 0.23 and 0.05 V vs Li/Li^+, respectively. The plot at initial voltage (3.1 V) is an almost straight line before the lithium ions were intercalated into the carbon electrode, implying that the system contained only a bulk solution resistance. As intercalation progressed, an increasingly large semicircle appears. This suggests that the total interfacial resistance increased as intercalation continued. In addition, it also indicates that the carbon electrode contacting the electrolyte was not initially covered with the passive film. However, the carbon electrode was finally covered with the passive film due to reduced EC, with the total interfacial resistance reaching 1240 $\Omega\,cm^2$ after a complete intercalation. As shown in Table 1, R_4 is the dominant resistance of the interface. Other studies also indicate that the properties of the passive film near the solution strongly influences the interface between the passive film and the electrolyte [3, 20, 21]. Moreover, the increase in the outer resistance (R_4) is larger than that of the inner resistance (R_i). According to Aurbach [18–20], the layer of the passive film near the solution is of porous structure; this becomes compact in the vicinity of the electrode. The compact part has a relatively dense

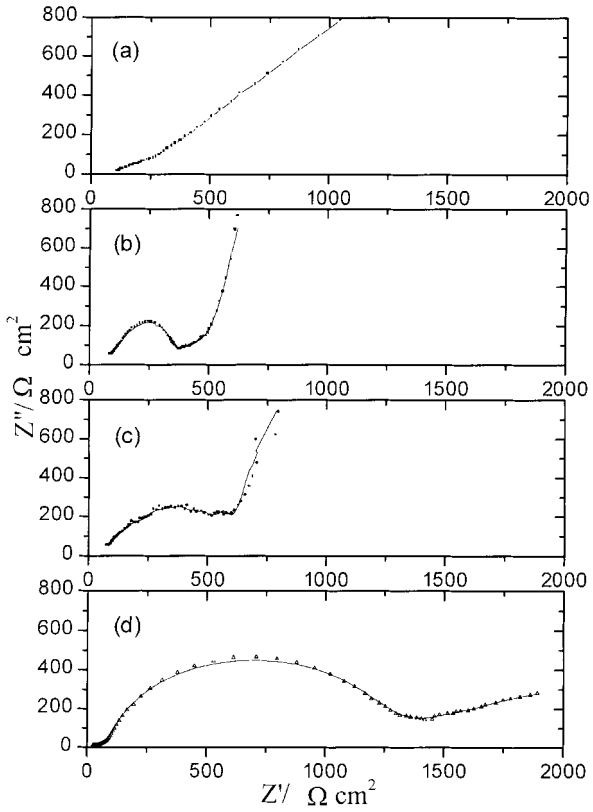

Fig. 2. Nyquist plot measured at OCV: (a) 3.1, (b) 0.64, (c) 0.23 and (d) 0.05 V vs Li/Li^+ in EC/1 M $LiPF_6$ electrolyte.

structure that grows with decreasing OCV. The thickness of the passive film (d_i) was calculated to be of the order of 10 nm, as shown in Table 1. Moreover, an increase in d_i also causes R_i to increase. It is clear that in the latter stage of intercalation R_4 increases rapidly, implying an intense reaction of EC on the electrode in this stage. Finally, the passive film grew to as thick as 89 nm after intercalation and became highly resistant. Lithium ions could no longer intercalate into the carbon electrode in the second cycle. Therefore, single EC solvent is not suitable for lithium ion batteries.

Figure 3(a–d) shows the Nyquist plots obtained in the DEC/1 M $LiPF_6$ electrolyte system during the first

Table 1. Resistance, capacitance, and thickness of the passive film on carbon electrode for single solvent systems

OCV/V vs Li/Li^+	EC/1 M $LiPF_6$			DEC/1 M $LiPF_6$			DMC/1 M $LiPF_6$		
	0.64 V	0.23 V	0.05 V	0.57 V	0.22 V	0.05 V	0.54 V	0.24 V	0.05 V
$R_4/\Omega\,cm^2$	134	189	711	98	89	55	65	93	168
$R_i/\Omega\,cm^2$	178	310	489	46	43	37	64	109	223
$R_{total}/\Omega\,cm^2$	366	540	1240	197	162	100	139	208	400
$C_1/\mu F$	2.6	0.97	0.7	7.9	20.4	42.8	32.4	3.0	1.9
$C_2/\mu F$	11.8	7.7	1.4	32.4	35.3	104.9	83	60.4	19.9
$C_3/\mu F$	71	20.6	10.8	65.3	83	332	306	221	22
$C_4/\mu F$	3800	1800	2000	1900	1500	3000	880	550	250
$C_5/\mu F$	80000	3400	6800	8600	48000	63000	1320	1560	1110
d_i^*/nm	19.56	48.32	89.0	6.88	3.56	1.43	1.84	14.17	24.78

* $d_i = \sum_{j=1}^{3} d_j$ where d_i is the thickness of compact passive film) [18, 19] and d_j is the thickness of the jth layer of the passive film and is derived from $d_j = \varepsilon_0 \varepsilon A / C_j$ (ε_0: permittivity of vacuum, ε: general permittivity = 5, A: electrode area, C_j: the capacitance for the jth layer of the passive film.)

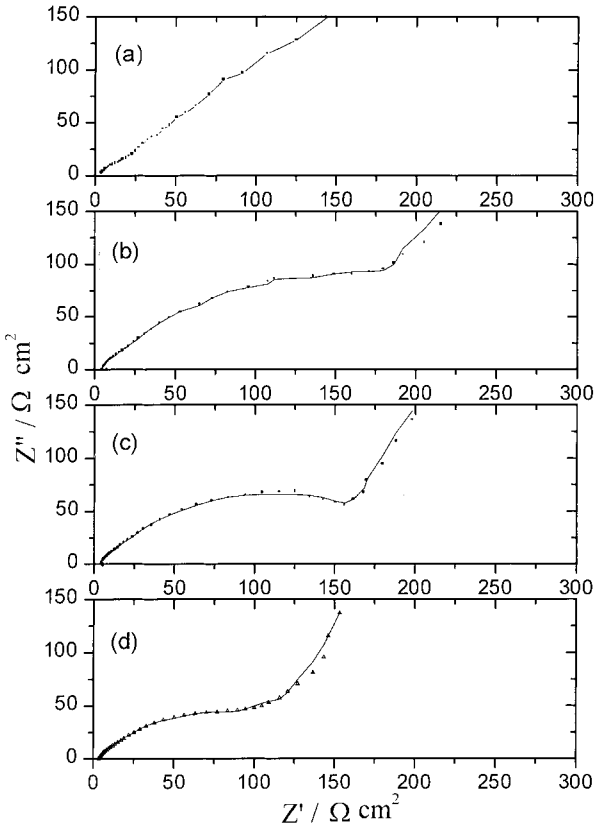

Fig. 3. Nyquist plot measured at OCV: (a) 3.1, (b) 0.57, (c) 0.22 and (d) 0.05 V vs Li/Li^+ in DEC/1 M $LiPF_6$ electrolyte.

intercalation. The OCVs for Figures 3 were 3.1, 0.57, 0.22 and 0.05 V vs Li/Li^+, respectively. As can be seen, the semicircle became smaller as intercalation progressed. This situation was just the opposite as compared to the EC solvent system. The total interfacial resistance in this case was about 100 Ω cm^2, which was much smaller than that of the EC solvent system, by about one order of magnitude. These findings imply that the DEC solvent system is more appropriate for lithium ion batteries than the EC solvent system. As indicated in Table 1, since R_4 is larger than R_i, it is the primary part of the total interfacial resistance. It was also found that R_i is almost constant during the intercalation process (46 to 37 Ω cm^2), therefore the decrease in total interfacial resistance shown in Figure 3 can be mainly attributed to the decrease in R_4. Interestingly, although R_i of the DEC/1 M $LiPF_6$ solvent system remained unchanged, d_i decreased continuously from 6.88 to 1.43 nm. In our previous study [22], we found significant gas formation, primarily CO and C_2H_6, which occurred only in the DEC system. One possible explanation is that the structure of the newly formed passive film is not stable in the DEC solvent system and could be squeezed to form a more compact structure during further intercalation. Hence, the passive film of the DEC system became thinner after complete intercalation. Consequently, the porosity of the outer passive film decreased as compression progressed. The fact that the relative proportion of R_4 to the total resistance of the interface decreased with decreasing OCV also suggests that the structure of the passive film becomes more compact as intercalation proceeds.

Figure 4 shows the Nyquist plot of the DMC/1 M $LiPF_6$ system when lithium ions were intercalated into the carbon electrode in the first half-cycle. The OCVs of Figure 4(a–d) were 3.1, 0.54, 0.24 and 0.05 V vs Li/Li^+, respectively. These clearly indicate that the total interfacial resistance and the thickness of the passive film increased as intercalation progressed. After the intercalation, the total interfacial resistance was about 400 Ω cm^2. The data in Table 1 indicate that R_4 was again the primary factor, as in the case of the EC or DEC solvent system. The only difference is that, as intercalation progressed, the total interfacial resistance and the thickness of the passive film decreased in the DEC solvent system, but increased in the EC or DMC solvent system.

Figure 5 shows the Nyquist plot of the EC/DEC/1 M $LiPF_6$ system with lithium ions being intercalated into the carbon electrode in the first half-cycle. The OCVs of Figure 5(a–d) were 3.1, 0.65, 0.23 and 0.05 V vs Li/Li^+, respectively. Apparently, in this binary solvent system the total interfacial resistance decreased as intercalation progressed, and after intercalation the total interfacial resistance had reached about 32 Ω cm^2. Table 2 shows that both R_i and R_4 decreased as intercalation progressed. Furthermore, the proportion of R_4 to the total interfacial resistance is relatively small. Thus, R_4 no longer dominated the total interfacial resistance. This

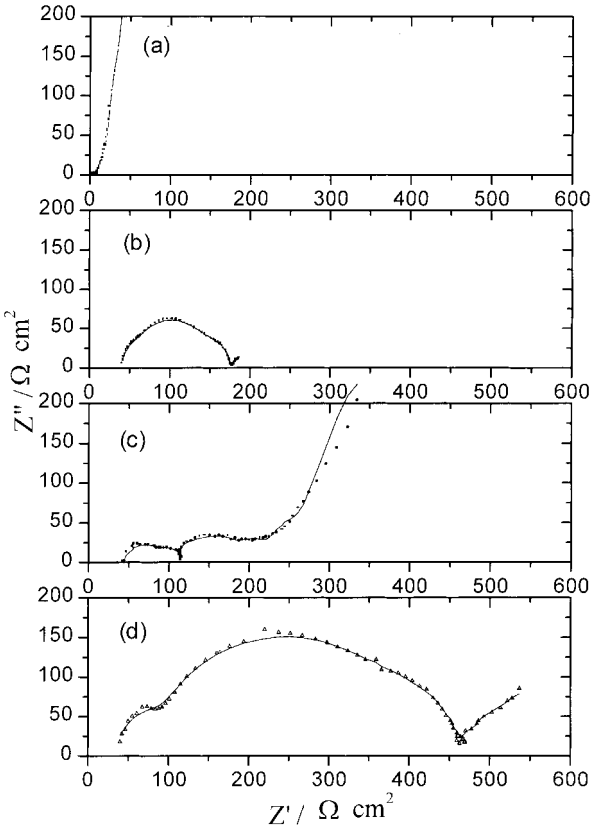

Fig. 4. Nyquist plot measured at OCV: (a) 3.1, (b) 0.54, (c) 0.24 and (d) 0.05 V vs Li/Li^+ in DMC/1 M $LiPF_6$ electrolyte.

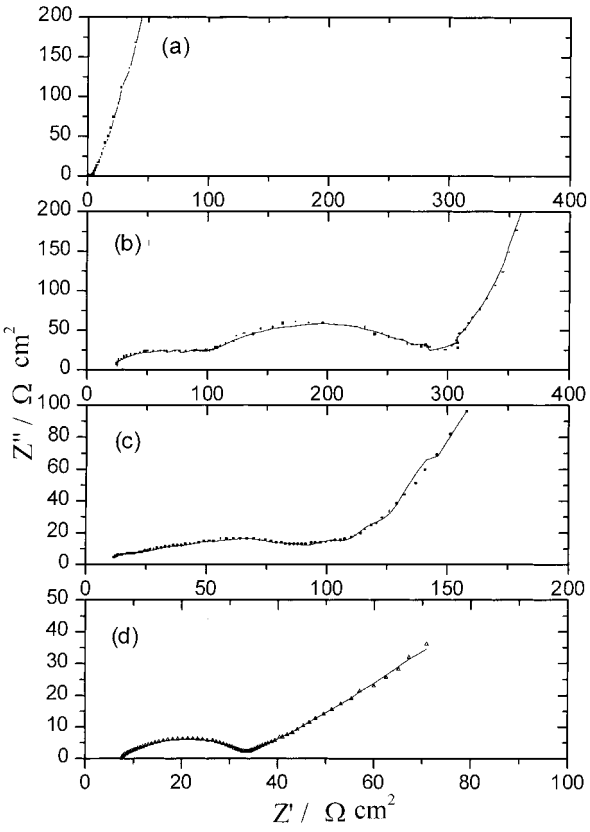

Fig. 5. Nyquist plot measured at OCV: (a) 3.1, (b) 0.65, (c) 0.23 and (d) 0.05 V vs Li/Li^+ in EC/DEC/1 M $LiPF_6$ electrolyte.

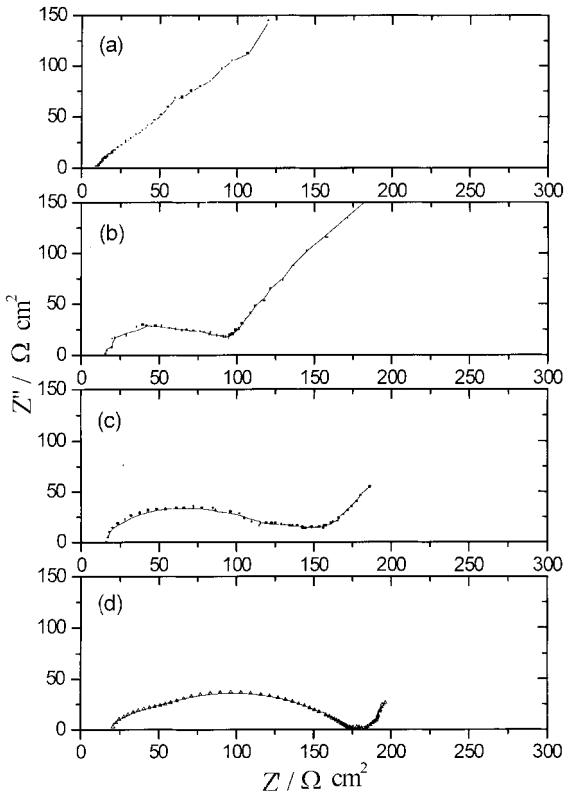

Fig. 6. Nyquist plot measured at OCV: (a) 3.1, (b) 0.61, (c) 0.25 and (d) 0.05 V vs Li/Li^+ in EC/DMC/1 M $LiPF_6$ electrolyte.

trend, which is drastically different from that of the EC, DEC or DMC single solvent systems, implies that the porous structure of a passive film is inhibited in a binary-solvent system. In fact, the thickness of the passive film became progressively thinner. This situation indicates that the physical properties of the passive film resemble those of the DEC solvent system. Our previous study [22] demonstrated that the chemical composition of the passive film in the EC/DEC binary-solvent system contained mainly reduction products of EC. However, according to the result of the impedance analysis, the property of the passive film is similar to that of a DEC system. This suggests that in the EC/DEC system, the physical structure of the passive film was strongly influenced by DEC which became very porous and compressible. Thus, during intercalation, the passive film forms a more compact structure.

Figure 6 shows the Nyquist plot of another binary solvent system, EC/DMC/1 M $LiPF_6$. The figure again shows that the total interfacial resistance increased as intercalation progressed. After intercalation, the total interfacial resistance was about 170 $\Omega\,cm^2$. In general, the passive film resistance and thickness in a binary-solvent system (EC/DEC or EC/DMC) is smaller than that in a single solvent system.

In this work, all the impedance studies were carried out in the first cycle. It would be informative to discover if the trend obtained prevails as cycling continues. It is apparent from Figure 7 that the film resistance to the EC/DEC system was significantly smaller than that of the EC/DMC system. Therefore, the EC/DEC system is

Table 2. Resistance, capacitance, and thickness of the passive film on carbon electrode for binary solvent systems

OCV/V vs Li/L^+	EC/DEC/1 M $LiPF_6$			EC/DMC/1 M $LiPF_6$		
	0.65 V	0.23 V	0.05 V	0.61 V	0.25 V	0.05 V
$R_4/\Omega\,cm^2$	33	24	5.4	33	32	36
$R_i/\Omega\,cm^2$	194	49	24.7	82	92	124
$R_{total}/\Omega\,cm^2$	228	95	32	116	132	170
$C_1/\mu F$	4.2	6.5	60	9.2	7.3	4.6
$C_2/\mu F$	78.1	84.8	250	45.3	33.8	30
$C_3/\mu F$	1000	800	800	306.5	142.3	100
$C_4/\mu F$	1200	4670	1800	1000	310	150
$C_5/\mu F$	1350	7300	3300	4440	800	200
d_i/nm	10.04	6.649	0.87	5.32	6.94	10.39

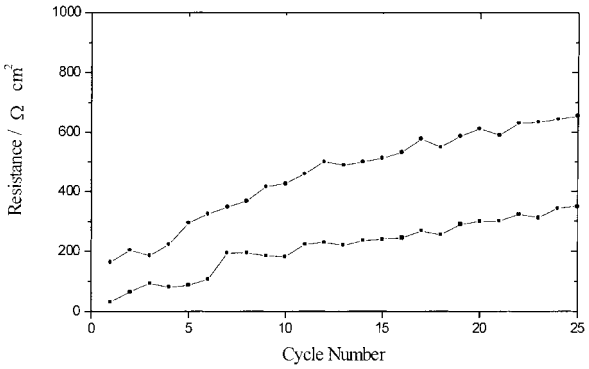

Fig. 7. Variation of interfacial resistance in binary solvent systems upon cycling. Conditions: charge at 0.25 mA cm^{-2}, cutoff 1.6 V; discharge at 0.25 mA cm^{-2}, cutoff 0.05 V. Key: (●) EC/DMC/1 M $LiPF_6$; (■) EC/DEC/1 M $LiPF_6$.

a better choice than the EC/DMC system for electrolyte preparation. Another noteworthy fact is that the resistance continuously increases with cycling, although it tends to level off after 25 cycles.

4. Conclusions

The following conclusions are now made regarding the passive film after the first cycle of intercalation:

(i) This approach, using five parallel RC circuits in series, can accurately simulate the change in resistance of the passive film when lithium ions are intercalated into a carbon electrode during the first cycle.

(ii) The porous structure of the passive film is the main factor controlling the interfacial resistance between carbon electrode and electrolyte in single solvent systems such as EC, DEC or DMC. However, the physical structure of these passive films becomes more compact in DEC-based electrolytes as intercalation progresses.

(iii) The passive film resistance in EC/DEC and EC/DMC systems is found to be lower than that in the corresponding single-solvent systems, which also implies that a thinner film is formed in the binary-solvent system. Moreover, in contrast to a single solvent system, the porous part of the passive film does not significantly influence the interfacial resistance.

References

1. G.B. Li, R.J. Xue, L.Q. Chen and Y.Z. Huang, *J. Power Sources* **54** (1995) 271.
2. M. Inaba, H. Yoshida, Z. Ogumi, T. Abe, Y. Mizutani and M. Asano, *J. Electrochem. Soc.* **142** (1995) 20.
3. Z.X. Shu, R.S. McMillan and J.J. Murray, *J. Electrochem. Soc.* **140** (1993) 922.
4. O. Chusid, Y. Ein-Eli, D. Aurbach, M. Babai and Y. Carmeli, *J. Power Sources* **43** (1993) 47.
5. K. Tatsumi, K. Zaghib, H. Abe, S. Higuchi, T. Ohsaki and Y. Sawada, *J. Power Sources* **54** (1995) 425.
6. H. Abe, K. Zaghib, K. Tatsumi and S. Higuchi, *J. Power Sources* **54** (1995) 236.
7. J.M. Chen, C.Y. Yao, C.H. Cheng, W.M. Hurng and T.H. Kao, *J. Power Sources* **54** (1995) 494.
8. D. Aurbach, Y. Ein-Eli, O. Chusid, Y. Carmeli, M. Babai and H. Yamin, *J. Electrochem. Soc.* **141** (1994) 603.
9. B. Simon, J.P. Boeuve and M. Broussely, *J. Power Sources* **43** (1993) 65.
10. J.O. Besenhard, M.W. Wagner, M. Winter, A.D. Jannakoudakis, P.D. Jannakoudakis and E. Theodoridou, *J. Power Sources* **44** (1993) 413.
11. K. Zaghib, K. Tatsumi, H. Abe, T. Ohsaki, Y. Sawada and S. Higuchi, *J. Power Sources* **54** (1995) 435.
12. D. Aurbach, Y. Ein-Eli, B. Markovsky, A. Zaban, S. Luski, Y. Carmeli and H. Yamin, *J.Electrochem. Soc.* **142** (1995) 2882.
13. E. Peled, *J. Electrochem. Soc.* **126** (1979) 2047.
14. D. Aurbach and A. Zaban, *J. Electroanal. Chem.* **348** (1993) 155.
15. D. Aurbach and A. Zaban, *J. Electroanal. Chem.* **367** (1994) 15.
16. N. Takami, A. Satoh, M. Hara and I. Ohsaki, *J. Electrochem. Soc.* **142** (1995) 371.
17. J.R. McDonald, *Impedance Spectroscopy*, Wiley Interscience, New York (1987).
18. D. Aurbach and A. Zaban, *J. Electrochem. Soc.* **141** (1994) 1808.
19. A. Zaban and D. Aurbach, *J. Power Sources* **54** (1995) 289.
20. D. Aurbach and Y. Gofer, *J. Electrochem. Soc.* **138** (1991) 3529.
21. K. Kanamura, H. Tamura and Z. Takehara, *J. Electroanal. Chem.* **333** (1992) 127.
22. C.R. Yang, Y.Y. Wang and C.C. Wan, *J. Power Sources* **72** (1998) 66.